Analytic expression for the short-time rate of growth of the intermaterial contact perimeter in two-dimensional chaotic flows and Hamiltonian systems

Alessandra Adrover,[1] Massimiliano Giona,[1,*] Fernando J. Muzzio,[2] Stefano Cerbelli,[2] and Mario M. Alvarez[2]

[1]*Centro Interuniversitario sui Sistemi Disordinati e sui Frattali nell'Ingegneria Chimica c/o Dipartimento di Ingegneria Chimica, Università di Roma ''La Sapienza,'' via Eudossiana 18, 00184 Roma, Italy*

[2]*Department of Chemical and Biochemical Engineering, Rutgers University, P.O. Box 909, Piscataway, New Jersey 08855-0909*

(Received 27 October 1997)

This article derives an analytic expression for the short- or intermediate-time behavior of the moment hierarchy of finite-time Liapunov exponents (stretching exponents) for two-dimensional periodically forced Hamiltonian systems and incompressible time-periodic fluid flows. As a result, the exponent characterizing the apparent short-time exponential growth of the intermaterial contact perimeter for two-dimensional systems can be predicted from the statistical properties of the invariant stretching distribution. The analysis as a whole is in fact grounded on an analytic expression for the high stretching tail of the invariant distribution of the finite-time Liapunov exponents. The asymptotic behavior of the moment hierarchy of the stretching field is also addressed in order to highlight the role of the dynamic heterogeneity accounted for by the variance of the stretching exponents. [S1063-651X(98)02807-4]

PACS number(s): 47.52.+j, 05.45.+b, 05.90.+m

I. INTRODUCTION

Recent articles [1–3] focusing on the evolution of the spatial structures generated by advection in chaotic flows have shown that the formation of partially mixed structures in time-periodic flows depends on two main interrelated factors: (1) the global increase of the intermaterial contact area (and the corresponding decrease of the characteristic length scale between material elements, referred to as striations for short), and (2) the degree of heterogeneity in the spatial distribution of the intermaterial contact area.

Despite the intense investigation of chaotic flows over the last decade, oriented mainly towards the characterization of stretching statistics [4–6] and the qualitative description of the role of the unstable manifold in the formation of coherent structures [7,8], a quantitative theory has yet to be developed for the time evolution of the intermaterial contact area and the spatial distribution of partially mixed structures.

Contrary to the general belief that the fundamental exponent controlling the temporal behavior of dynamic quantities in mixing systems (such as the intermaterial contact area or the average characteristic length scale between striations) is the Liapunov exponent [4], Alvarez *et al.* [3] have recently shown by means of numerical simulations on a two-dimensional area-preserving and differentiable model system that the intermaterial contact area (or more precisely the intermaterial contact perimeter, since $d=2$) scales exponentially with the number of flow periods n (henceforth referred to as iterations), but with an exponent θ which is unambiguously different from and greater than the Liapunov exponent Λ. A short-time exponential growth faster than $\exp(\Lambda n)$, as predicted by the asymptotic Liapunov scaling, has also been numerically observed by Beigie *et al.* [1], and attributed to the non-Gaussian nature of the stretching distribution.

The aim of this article is to provide a quantitative estimate of the rate of growth of the intermaterial contact area in chaotic flow systems for short- and intermediate-time scales.

The analysis of the rate of growth of interfaces evolving within the chaotic region in two-dimensional (2D) time-periodic flows finds its direct application in the study of mixing process in fluid flows, when the stretching of an interface between two fluid species affects the rate of mixing, and of the kinetic-dynamo phenomena, when the stretching of fluid elements affects magnetic field amplification. In particular, the short- or intermediate-time scales are those relevant in fluid-mixing applications.

Indeed, mixing of fluids takes place by a combination of different mechanisms such as stirring, stretching, folding, and diffusion, the latter one promoting uniformity at small length scales. If the viscosity is high enough to ensure creeping-flow conditions, then diffusion effects can be neglected at the early stage of the mixing process. Henceforth, a purely kinematic approach to a real mixing system (such as the analysis of the stretching of the fluid-fluid interface) makes sense at short- or intermediate-time scales, i.e., as far as the characteristic length scales controlled by convection are larger than the diffusive-length scales.

In this article we derive an analytic expression for the short- or intermediate-time behavior of the moments of the stretching field $M(m;n)=\langle(\lambda^{(n)})^m\rangle$ (where $m=1,2,3,\ldots$, and $\langle\ \rangle$ indicates the average with respect to the ergodic invariant measure within the chaotic region), which for $m=1$ coincides with the scaling of the length of a generic material filament. Attention is focused on two-dimensional, continuous, and differentiable periodically forced Hamiltonian systems and incompressible time-periodic fluid flows.

The present analysis is based on the application of a global invariant rescaling of the spectrum of finite-time Li-

*Permanent address: Dipartimento di Ingegneria Chimica Università di Cagliari, piazza d'Armi, 09123 Cagliari, Italy.

 © 1998 The American Physical Society

apunov exponents recently proposed in [9] (see Sec. IV for details). We show analytically that the mth order moment of the stretching exponents ($m=1,2,\ldots$) grows at short or intermediate time faster than the exponential behavior predicted by the Liapunov scaling $\exp(nm\Lambda)$, although the short-time scaling behavior may be not strictly exponential, being given by the product of an exponential term and a stretched exponential contribution. The enhanced exponential growth observed at short time is a nonpersistent feature of the flow, since the asymptotic exponential behavior of $M(m;n)$ is definitely controlled by Λ (under the condition of differentiability of the Poincaré map of the flow), e.g., $\lim_{n\to\infty}\ln M(m;n)/n=m\Lambda$, as predicted by the Oseledec theorem [10].

The analysis of the stretching statistics for high values of the iteration n is rendered more accurate in numerical terms by making use of the invariant definition of stretching related to the characteristic (and invariant) asymptotic directions of the unstable manifold, thus defining the concept of elongation [11]. For this reason, the relation between the invariant geometric properties and the statistical characterization of the stretching dynamics are addressed in Sec. II.

The article is organized as follows. Section II briefly reviews the geometric properties of the unstable manifold and their implications in the description of the stretching or elongation dynamics. Section III shows the numerical results for the rate of growth of the intermaterial contact perimeter and the scaling of higher-order moments $M(m;n)$ by analyzing several characteristic model systems (standard map, Duffing oscillator, sine flow, flow between eccentric cylinders). The connection between intermaterial contact length and the ergodic average of the stretching field is also addressed. Section IV describes the statistical properties of the stretching field which are relevant in the analysis of short-time scaling. Specifically, the expression for the invariant probability density function of the stretching exponents derived by Adrover *et al.* [9] is reviewed and the scaling properties of the variance of the stretching exponent are discussed. The invariant rescaling suggested in [9] does in fact express the high stretching tail of the distribution as a function solely of the variance of the stretching field. Application of the invariant rescaling mentioned above makes it possible to derive an analytic expression for the short-time scaling of $M(m;n)$ and to obtain the range of time scales up to which this nonpersistent scaling occurs (Sec. V). Comparison with numerical results for several dynamical systems is addressed in Sec. VI. Finally, Sec. VII discusses the asymptotic scaling of $M(m;n)$ and the influence of stretching heterogeneity on asymptotic behavior.

II. STRETCHINGS, ELONGATIONS, AND THE INVARIANT GEOMETRIC STRUCTURE OF THE UNSTABLE MANIFOLD

Throughout this article, two-dimensional time-periodic Hamiltonian systems and incompressible chaotic flows are investigated either by analyzing the associated Poincaré maps, Φ, or through direct reference to two-dimensional maps which can be regarded as explicit Poincaré sections of some continuous-time flow. We shall also assume that Φ and its inverse are both continuous and differentiable, and thus define a diffeomorphism, and that Φ is chaotic within an invariant submanifold $\mathcal{C}_c$, referred to as the chaotic region.

As a starting point, let us consider the evolution of a generic continuous material filament (one-dimensional set of initial conditions) initially located within the chaotic region. As extensively discussed elsewhere (see [2], and references therein), the evolution of material lines in two-dimensional time-periodic chaotic flows possesses global invariant geometric features, and convergence towards these invariant patterns occurs after few iterations [3]. From a qualitative point of view, this phenomenon is due to the dominating role of the unstable manifold [7,8]. A quantitative description of this geometric invariance can be achieved by introducing the concept of *asymptotic directionality* [11], which is a characteristic property of two-dimensional chaotic area-preserving diffeomorphisms.

Let us assume that Φ is a diffeomorphism which is chaotic within a submanifold $\mathcal{C}_c$, the chaotic region. The invariant orientational properties of the map Φ are fully described by a vector field $\{\mathbf{e}_\infty^u(\mathbf{x})\}$ tangent at each point $\mathbf{x}\in\mathcal{C}_c$ to the unstable manifold $\mathcal{W}^u$. The vector $\mathbf{e}_\infty^u(\mathbf{x})$ can be obtained as the limit of the unstable eigenvector of the Jacobian matrix of the nth-order map evaluated at the nth-order preimage of the point $\mathbf{x}$:

$$\Phi^{n*}(\Phi^{-n}(\mathbf{x}))\mathbf{e}_n^u(\mathbf{x})=\lambda^{(n)}(\mathbf{x})\mathbf{e}_n^u(\mathbf{x}), \tag{1}$$

$$\mathbf{e}_\infty^u(\mathbf{x})=\lim_{n\to\infty}\mathbf{e}_n^u(\mathbf{x}), \tag{2}$$

where $\Phi^*(\mathbf{x})=\partial\Phi/\partial\mathbf{x}$ is the Jacobian matrix of Φ, $\Phi^{n*}(\Phi^{-n}(\mathbf{x}))=\partial\Phi^n(\mathbf{x})/\partial\mathbf{x}|_{\mathbf{x}=\Phi^{-n}(\mathbf{x})}=\Pi_{j=1}^n\Phi^*(\Phi^{-j}(\mathbf{x}))$, and $\lambda^{(n)}(\mathbf{x})$ is a diverging sequence of eigenvalues (equivalent to the stretching at point $\mathbf{x}$). [In determining the limit in Eq. (1), some precautions should be taken, namely, that all the $\mathbf{e}_n^u(\mathbf{x})$ are unit vectors and that their x component should be non-negative. This is because the convergence of $\mathbf{e}_n^u(\mathbf{x})$ towards $\mathbf{e}_\infty^u(\mathbf{x})$ is, strictly speaking, a convergence of eigenspaces.]

It has been shown that the vector $\mathbf{e}_n^u(\mathbf{x})$ converges towards $\mathbf{e}_\infty^u(\mathbf{x})$ for each $\mathbf{x}$ within the chaotic region, and that the direction spanned by $\mathbf{e}_\infty^u(\mathbf{x})$ coincides with the asymptotic direction attained by the tangent to a material line at $\mathbf{x}$ advected by the flow [11]. Let $\mathcal{E}_\mathbf{x}^u$ be the (one-dimensional) vector subspace spanned by $\mathbf{e}_\infty^u(\mathbf{x})$. The unstable (dilating) subspaces $\mathcal{E}_\mathbf{x}^u$ defined for each $\mathbf{x}\in\mathcal{C}_c$ are related to each other by the equation

$$\mathcal{E}_{\Phi(\mathbf{x})}^u=\Phi^*(\mathbf{x})\mathcal{E}_\mathbf{x}^u, \tag{3}$$

which means that if $\mathbf{y}^u\in\mathcal{E}_\mathbf{x}^u$, then $\Phi^*(\mathbf{x})\mathbf{y}^u\in\mathcal{E}_{\Phi(\mathbf{x})}^u$.

By making use of the invariant properties of Φ expressed by the field of vectors $\{\mathbf{e}_\infty^u(\mathbf{x})\}$, the stretching dynamics induced by Φ can be conveniently described in terms of the *elongations* $\lambda_e^{(n)}(\mathbf{x})$. The elongation $\lambda_e^{(n)}(\mathbf{x})$ is the stretching experienced after n iterations at the point $\mathbf{x}$ along the asymptotic unstable directions (tangent to the unstable manifold), i.e.,

$$\lambda_e^{(n)}(\mathbf{x}) = \frac{||\Phi^{n*}(\mathbf{x})\mathbf{y}^u||}{||\mathbf{y}^u||}, \quad \mathbf{y}^u \in \mathcal{E}_{\mathbf{x}}^u \tag{4}$$

where $||\ ||$ indicates vector norm. The definition of elongation is similar to that of stretching $\lambda^{(n)}(\mathbf{x})$, defined as $\lambda^{(n)}(\mathbf{x}) = ||\Phi^{n*}(\mathbf{x})\ \mathbf{l}(0)||/||\mathbf{l}(0)||$, where $\mathbf{l}(0)$ is an arbitrarily oriented initial vector [4]. However, while the elongation $\lambda_e^{(n)}$ is strictly speaking a field, depending on space $\mathbf{x}$ and time n, the stretching $\lambda^{(n)}(\mathbf{x})$ also depends on the orientation of the initial vector, and is therefore not uniquely specified by $\mathbf{x}$ and by the number of iterations n. Despite this conceptual difference, the scaling properties of stretchings and elongations are the same because arbitrarily oriented vectors converge exponentially towards the asymptotic field of unstable directions spanned by the field $\{\mathbf{e}_\infty^u(\mathbf{x})\}$. For this reason, we shall henceforth use elongations and stretchings as synonymous terms in the analysis of statistical properties.

The *elongation exponent* $a_n(\mathbf{x})$ can be defined as the natural logarithm of the elongation, $a_n(\mathbf{x}) = \ln[\lambda_e^{(n)}(\mathbf{x})]$. The definition of elongation given by Eq. (4) is particularly useful in theoretical analysis. It follows in fact from the recursive relation between invariant unstable subspaces $\{\mathcal{E}_{\mathbf{x}}^u\}$, Eq. (3), that the n-step elongation exponent $a_n(\mathbf{x})$ can be expressed as the summation of the one-step elongation exponents $a_1(\mathbf{x})$ along a particle trajectory starting from $\mathbf{x}$ [11–13], i.e.,

$$a_n(\mathbf{x}) = \sum_{j=0}^{n-1} a_1(\mathbf{x}_j(\mathbf{x})), \quad \mathbf{x}_j(\mathbf{x}) = \Phi^j(\mathbf{x}). \tag{5}$$

Equation (5) shows that the stretching dynamics is strictly a multiplicative process once expressed with respect to the invariant basis $\{\mathbf{e}_\infty^u(\mathbf{x})\}$. It also gives a convenient way to estimate $a_n(\mathbf{x})$ [and analogously the finite-time Liapunov exponent defined as $h(\mathbf{x};n) = a_n(\mathbf{x})/n$] numerically as the superposition of the one-step elongation exponents.

Let us use $\langle\ \rangle$ to denote the ensemble average with respect to the uniform ergodic invariant measure within the chaotic region $\mathcal{C}_c$. As a consequence of Eq. (5), it follows that

$$\langle a_n \rangle = \langle \ln \lambda_e^{(n)} \rangle = n\Lambda \simeq \langle \ln \lambda^{(n)} \rangle, \tag{6}$$

$$\begin{aligned}\sigma_a^2(n) &= \langle (a_n - n\Lambda)^2 \rangle \\ &= \sum_{j=0}^{n-1} \sum_{k=0}^{n-1} \langle [a_1(\mathbf{x}_j(\mathbf{x})) - \Lambda][a_1(\mathbf{x}_k(\mathbf{x})) - \Lambda] \rangle \\ &\simeq \langle\langle (\ln \lambda^{(n)} - \langle \ln \lambda^{(n)} \rangle)^2 \rangle\rangle,\end{aligned} \tag{7}$$

where Λ is the Liapunov exponent.

III. RATE OF GROWTH OF INTERMATERIAL CONTACT LENGTH

We shall now analyze the evolution of the intermaterial contact length $L^{(n)}$ after n iterations by considering an initial regular curve γ_0 of length $L^{(0)}$, parametrized with respect to a real parameter p, i.e., $\gamma_0 = \{\mathbf{x} = (x,y) | \mathbf{x} = \mathbf{x}_0(p), p \in [0,1]\}$. After n iterations, γ_0 evolves into a new segment $\gamma_n = \{\mathbf{x}_n(p) = \Phi^n(\mathbf{x}_0(p)),\ p \in [0,1]\}$, the length of which is given by $L^{(n)}$,

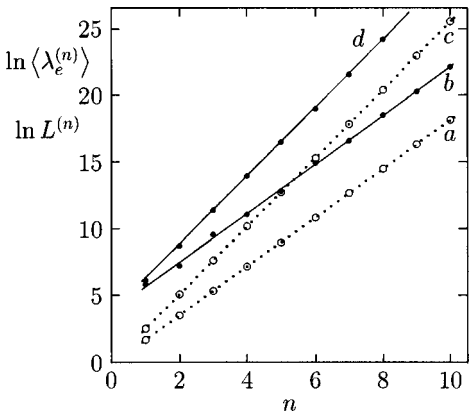

FIG. 1. Comparison of $\ln\langle\lambda_e^{(n)}\rangle$ (dotted lines) and the natural logarithm of the intermaterial contact length $\ln L^{(n)}$ (solid lines) vs n for an arbitrary initial filament γ_0 lying within the chaotic region $\mathcal{C}_c$ for two different dynamical systems. (a),(b) Sine flow, $T = 0.6$; (c), (d) standard map, $T = 20$. Lines (a) and (b) [and analogously lines (c) and (d)] have the same slope.

$$\begin{aligned}L^{(n)} &= \int_0^1 \left|\left| \frac{d\mathbf{x}_n(p)}{dp} \right|\right| dp \\ &= \int_0^1 \left|\left| \left.\frac{\partial \Phi^n(\mathbf{x})}{\partial \mathbf{x}}\right|_{\mathbf{x}=\mathbf{x}_0(p)} \frac{d\mathbf{x}_0(p)}{dp} \right|\right| dp.\end{aligned} \tag{8}$$

The quantity appearing within the integral in Eq. (8) is proportional to the local stretching $\lambda^{(n)}(\mathbf{x}_0(p))$ after n iterations, evaluated at $\mathbf{x}_0(p)$. The intermaterial contact length $L^{(n)}$ can therefore be expressed as

$$L^{(n)} \simeq \int_0^1 \lambda^{(n)}(\mathbf{x}(p))\ dp = \langle \lambda^{(n)} \rangle_{\gamma_0} \simeq \langle \lambda_e^{(n)} \rangle_{\gamma_0}, \tag{9}$$

where $\langle\ \rangle_{\gamma_0}$ indicates that the average is performed over γ_0. By taking the average of Eq. (9) over all the possible one-dimensional curves embedded in the chaotic region, it follows that

$$L^{(n)} \sim \langle \lambda_e^{(n)} \rangle, \tag{10}$$

i.e., the scaling properties of the intermaterial contact length can be predicted by the scaling of the first-order moment $M(1;n)$ of the elongation field, averaged with respect to the ergodic invariant measure on $\mathcal{C}_c$.

The numerical validation of this result is shown in Fig. 1, which illustrates the comparison of the scaling behavior of $\ln\langle\lambda_e^{(n)}\rangle$ (dotted lines) and $\ln L^{(n)}$ vs n (continuous lines) for an arbitrary initial filament γ_0 and for two different dynamical systems on the torus: the sine-flow map [14]

$$\begin{aligned}x_{n+1} &= x_n + Tf(y_n + Tf(x_n)) \mod 1, \\ y_{n+1} &= y_n + Tf(x_n) \mod 1,\end{aligned} \tag{11}$$

with $f(x) = \sin(2\pi x)$, and the Chirikov standard map [15]

$$\begin{aligned}x_{n+1} &= x_n - (T/2\pi)\sin(2\pi y_n) \mod 1, \\ y_{n+1} &= y_n + x_{n+1} \mod 1,\end{aligned} \tag{12}$$

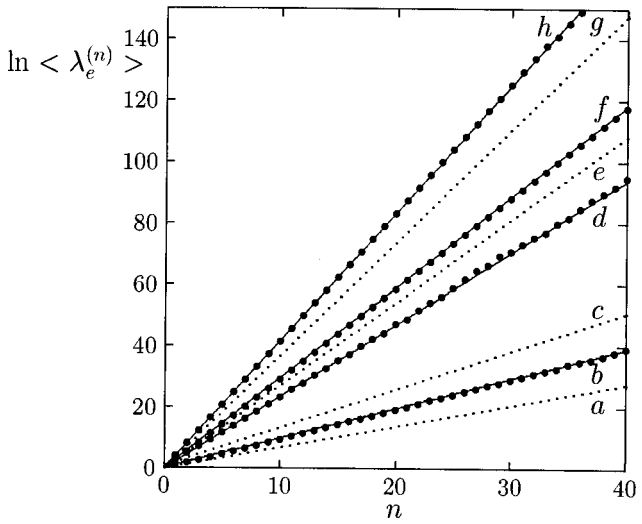

FIG. 2. Short-time behavior of $\langle \ln \lambda_e^{(n)} \rangle$ (dotted lines) and of $\ln \langle \lambda_e^{(n)} \rangle$ (dots) for several chaotic dynamical systems. The averages were performed over an ergodic trajectory of N_p tracer points within the chaotic region $\mathcal{C}_c$. (a),(b) Duffing oscillator, $\varepsilon = 2.35$, $\omega = 1$ ($N_p = 5 \times 10^5$); (c),(d) flow between eccentric cylinders, $\theta_{\text{out}} = (5\pi/2)$, ($N_p = 10^5$); (e),(f) standard map, $T = 30$ ($N_p = 10^7$); (g),(h) sine flow, $T = 2.0$ ($N_p = 10^7$). The solid lines show the exponential behavior $\ln \langle \lambda_e^{(n)} \rangle = \exp(n\theta)$, Eq. (13). The dotted lines show the exponential behavior for $\langle \ln \lambda_e^{(n)} \rangle = n\Lambda$.

for a value of $T > T_c \simeq 0.97$, where T_c is the characteristic value of the parameter, corresponding to the breakup of the last Kolmogorov-Arnold-Moser (KAM) torus for the standard map [16].

An important numerical implication of Eq. (10) is the following. The direct estimate of $L^{(n)}$ from its definition as the length of an evolved curve γ_n after n iterations, starting from γ_0, requires an iterative interpolation along the initial filament γ_0 in order to preserve its continuity [3]. As a result, the analysis is limited by computer resources, both in time and in memory, to low values of $n \simeq 8-12$. The estimate of the scaling of $L^{(n)}$ as the average of $\langle \lambda_e^{(n)} \rangle$ along an ergodic trajectory, Eq. (10), solves many numerical problems by making it possible to reach values of n of the order of $n = 200-300$, which it would otherwise have been impossible to investigate starting from the original definition, and to obtain accurate results in a reasonable span of computer time.

As several authors have already pointed out [1,3], the scaling behavior of $L^{(n)}$, or equivalently of $\langle \lambda_e^{(n)} \rangle$, can be approximated for small or intermediate values of n by means of an exponential law

$$L^{(n)} \sim \langle \lambda_e^{(n)} \rangle \sim e^{n\theta}, \tag{13}$$

where θ is an exponent definitely greater than Λ, the Liapunov exponent of the system. To give a numerical example, Fig. 2 shows the short-time behavior of $\ln(\langle \lambda_e^{(n)} \rangle)$, its linear fitting $\ln(\langle \lambda_e^{(n)} \rangle) \sim n\theta$ and the comparison with the linear scaling of $\langle \ln \lambda_e^{(n)} \rangle = n\Lambda$ controlled by the Liapunov exponent Λ for several dynamical systems, such as the sine-flow Eq. (11), the standard map Eq. (12), the Duffing oscillator [17]

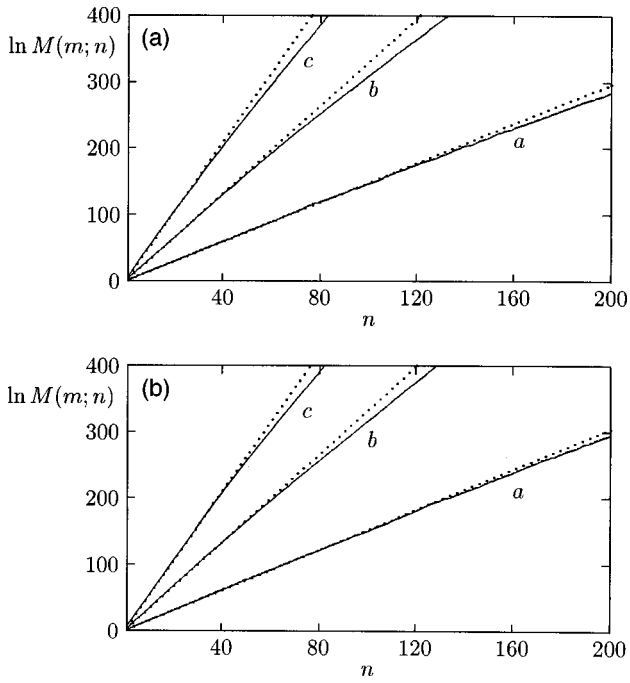

FIG. 3. $\ln M(m;n)$ vs n for two different dynamical systems. (a) $m = 1$; (b) $m = 2$; (c) $m = 3$. The dotted lines show the short-time exponential behavior $M(m;n) \simeq \exp[n\theta(m)]$, Eq. (15). (a) Sine flow ($T = 0.5$); (b) standard map ($T = 6.9115$).

$$\dot{x} = y,$$

$$\dot{y} = x - x^3 + \varepsilon \cos(\omega t), \tag{14}$$

and the flow between two eccentric corotating cylinders [5]. The latter system is a typical, physically realizable chaotic flow extensively used in laboratory and numerical experiments on chaotic mixing (see [4] for a review). In this system, the two cylinders rotate in a discontinuous time-periodic fashion in order to generate a chaotic flow [18]. Under creeping-flow conditions, a closed-form expression for the stream function is available [19]. The geometry of the apparatus is characterized by two parameters: $r = r_{\text{in}}/r_{\text{out}}$ (the ratio of the radius of the inner cylinder to that of the outer) and $ec = e/r_{\text{out}}$ (the dimensionless eccentricity) $ec = e/r_{\text{out}}$, given by the distance between the centers of the two cylinders divided by the radius of the outer cylinder. The flow protocol is parametrized by the rotation of the outer cylinder θ_{out} and by the ratio Ω of the rotation angle of the inner cylinder to that of the outer cylinder. The values $r = 1/3$, $ec = 3/10$, and $\Omega = 3$ are used here.

Let us now consider the higher-order moments of the stretching hierarchy $M(m;n)$. Such moments seem to exhibit a short- or intermediate-time exponential scaling with n,

$$M(m;n) = \langle (\lambda_e^{(n)})^m \rangle \sim \exp[n\theta(m)], \quad m = 1,2,3,\ldots \tag{15}$$

characterized by an exponent $\theta(m)$, always greater than the asymptotic exponent $m\Lambda$. By definition, for $m = 1$, $\theta(1) = \theta$ introduced in Eq. (13). Figure 3 shows the behavior of $\ln M(m;n)$ vs n for $m = 1,2,3$ for the sine flow ($T = 0.5$) and for the standard map ($T = 6.9115$) and its short-time lin-

ear fitting $\ln M(m;n) \sim n\theta(m)$. It can be observed that the exponential behavior expressed by Eq. (15) holds over a significant range of n, but as n increases beyond a certain value (characteristic for each system and depending upon the order m), the moments $M(m;n)$ start to deviate significantly from the initial scaling and move slowly towards the asymptotic behavior expressed by $\exp\{n[m\Lambda + o(n)]\}$, as predicted by the Oseledec theorem [10]. Moreover, the larger the order m, the smaller the n range of validity of Eq. (15) becomes. Although Eq. (15) does not hold asymptotically, the range of n for which it may be assumed to be valid, and the range of values attained by $M(m;n)$ (hundreds of decades) are indeed significantly large. Furthermore, the short- or intermediate-time scaling is of specific relevance in many fluid-mixing phenomena which involve transient processes.

It should be observed that we have so far used the term short- or intermediate-time scales in a fairly qualitative way, practically as the opposite of asymptotic long-term behavior. A quantitative estimate of the time scales up to which Eqs. (13) and (15) are valid will be given in Sec. VI once an analytical expression has been derived for the temporal behavior $M(m;n)$.

By anticipating a result that will be extensively discussed below (Sec. VI), Eq. (15) can be viewed as the manifestation of an important statistical feature characterizing all the mixing systems analyzed here: regardless of the functional form of the probability density function for stretching exponents, its variance $\sigma_a^2(n)$ is a monotonically increasing function of n diverging to infinity (see Sec. IV B). In actual fact, the only case for which $\langle (\lambda_e^{(n)})^m \rangle \sim \exp(nm\Lambda)$ at short- or intermediate-time scales is given by the family of K diffeomorphisms on the torus, which are topologically conjugate with the linear toral automorphism [20]. These systems are globally hyperbolic and are characterized by a uniform scaling exponent (coinciding with the Liapunov exponent). For such systems, $\sigma_a(n) = \sigma_K + o(n)$, and the variance therefore saturates towards a constant value $\sigma_K \geqslant 0$.

IV. STATISTICAL PROPERTIES OF THE ELONGATION FIELD

We have shown in Sec. III that the intermaterial contact length $L^{(n)}$ can be related to the temporal evolution of the stretching field, averaged with respect to the ergodic invariant measure, Eq. (10). This makes it possible to approach the study of the rate of growth of $L^{(n)}$ analytically by making use of the statistical properties characterizing the elongation field. The main statistical features of $\lambda_e^{(n)}$ which will be used to obtain an analytic expression for $\theta(m)$ are analyzed in this section.

A. Globally invariant rescaling of the elongation exponent spectra

The analysis of the invariant statistical properties of chaotic dynamical systems [21–24] and in particular of short-time Liapunov exponents (SLE) has been a subject of intense investigation in recent years [25]. Some invariant rescalings for SLE spectra have been proposed, most of them deriving from the original exponential rescaling suggested by Grassberger *et al.* [26]. A similar exponential rescaling was considered by Ott and Antonsen in the case of the incompressible generalized 2D Baker transformation [6], and although derived in the case of a noncontinuous map, this has since been taken as the general model for the invariant rescaling of stretching distributions in chaotic dynamical systems induced by the multiplicative nature of the stretching process. All the invariant rescalings so far proposed fail for the low stretching tail (i.e., for $a_n < n\Lambda$, i.e., for $h < \Lambda$) [12,27], which is strongly affected by the stickiness of quasiperiodic islands and cantori surrounding the chaotic region.

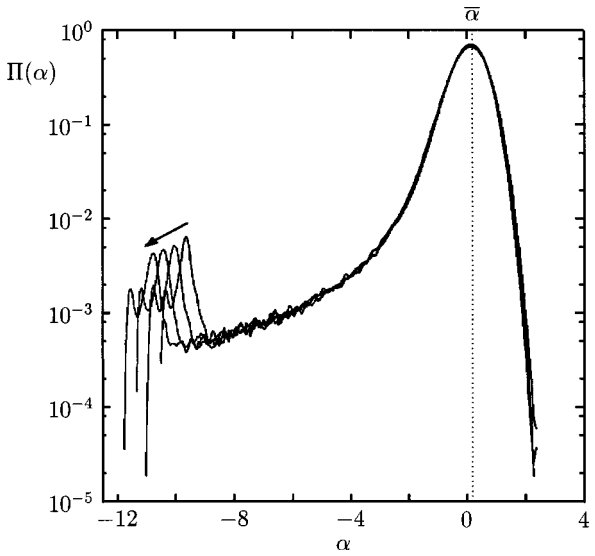

FIG. 4. $\Pi(\alpha)$ vs α for different values of n for the standard map at $T = 6.9115$. The arrow shows the direction of increasing values of $n = 150,175,200,225$. The dotted vertical line shows the value of the mode $\overline{\alpha}$. The simulations were performed over an ergodic trajectory within the chaotic region ($N_p = 10^7$ data points).

A globally invariant rescaling for the probability density function for the elongation (stretching) exponents $P(a_n;n)$ has recently been proposed [9] in the case of two-dimensional area-preserving chaotic maps:

$$P(a_n;n) = \frac{1}{\sigma_a(n)} \Pi\left(\frac{a_n - n\Lambda}{\sigma_a(n)} \right), \tag{16}$$

$\Pi(\alpha)$ being an invariant probability density function of the rescaled variable $\alpha = (a_n - n\Lambda)/\sigma_a(n)$, and $\sigma_a(n)$ the square root of the variance of the elongation exponents, Eq. (7). The invariant function $\Pi(\alpha)$ is a standardized probability density function possessing zero mean and unit variance. To give a numerical validation of Eq. (16), Fig. 4 shows the behavior of the invariant function $\Pi(\alpha)$ for a typical dynamical system (standard map). Numerical simulations confirm that $\Pi(\alpha)$ is globally invariant, i.e., the rescaling relation expressed by Eq. (16) holds also for negative values of α corresponding to the low-stretching region. The influence of quasiperiodic islands, elliptic points, and cantori, around which stretching is particularly low, shows itself as a hump for negative values of α (see Fig. 4). This hump moves towards more negative α and lower probability values as n increases, and progressively becomes smoother until it collapses into a single enveloping curve [9].

We shall use $\overline{\alpha}$ to denote the mode of α, i.e., the value corresponding to the maximum of $\Pi(\alpha)$, $\max_\alpha \Pi(\alpha)$

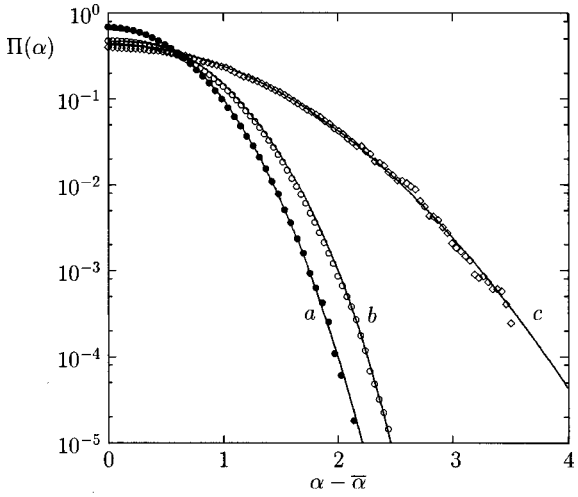

FIG. 5. $\Pi(\alpha)$ vs $(\alpha-\overline{\alpha})>0$. Comparison of the theoretical expression Eq. (17) with simulation results. (*a*) Standard map, $T=6.9115$; (*b*) sine flow, $T=0.6$; (*c*) Duffing oscillator, $\varepsilon=2.35$, $\omega=1.0$.

$=\Pi(\overline{\alpha})$, which is also the local maximum of $\Pi(\alpha)$. By enforcing Eq. (16) and by making use of a slight modification of the exponential rescaling proposed by Grassberger *et al.* [26], it is shown in [9] that for $\alpha\geqslant\overline{\alpha}$ the functional form of $\Pi(\alpha)$ attains the general expression

$$\Pi(\alpha)=\Pi(\overline{\alpha})\exp\left[-c_1\zeta^{-1}\left(\frac{\alpha-\overline{\alpha}}{c_2}\right)\right],\quad \alpha\geqslant\overline{\alpha} \tag{17}$$

where c_1 and c_2 are two constants and the function ζ^{-1} is the inverse function of $\zeta(n)$ defined by

$$\zeta(n)=n/\sigma_a(n). \tag{18}$$

Since $\zeta(n)$ is a monotonically increasing function of n, diverging to infinity as $n\to\infty$, it admits a global inverse function ζ^{-1}. Figure 5 shows the ln-normal plot of the positive tail of $\Pi(\alpha)$ vs $\alpha-\overline{\alpha}$ numerically estimated for several dynamical systems, and its excellent agreement with the theoretical expression Eq. (17).

Equation (17) indicates that the functional form of $\Pi(\alpha)$, for $\alpha>\overline{\alpha}$, is controlled by the fluctuational-correlation properties of the elongation field, expressed by the temporal behavior of the variance of the elongation exponents. The implications of this property are extensively addressed in Sec. VI of this article.

Another interesting feature of the invariant rescaling Eq. (16) is the fact that numerical simulations indicate the existence of a finite and constant upper bound $\alpha_{\max}$ of the support of $\Pi(\alpha)$ such that $\Pi(\alpha)=0$ for $\alpha>\alpha_{\max}$. As an example, Fig. 6 shows the behavior of $\alpha_{\max}^{(n)}$ vs n for the sine-flow map (for several values of the parameter T), $\alpha_{\max}^{(n)}$ being the value of $\alpha_{\max}$ associated with the nth-order approximation of $\Pi(\alpha)=\sigma_a(n)P(a_n;n)|_{a_n=n\Lambda+\alpha\sigma_a(n)}$. In point of fact, it is easy to show by enforcing the Oseledec theorem [10] that if $\Pi(\alpha)$ is a smooth function of α, then

$$\alpha_{\max}^{(n)}\leqslant Cn^{\nu}/\sigma_a(n),\quad 0\leqslant\nu<1 \tag{19}$$

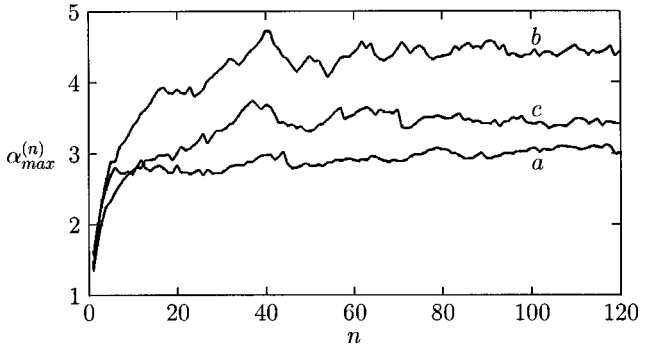

FIG. 6. $\alpha_{\max}^{(n)}$ vs n for the sine flow for several values of T; (*a*) $T=0.6$; (*b*) $T=0.8$; (*c*) $T=1.0$.

where C is a positive constant. Indeed, the results shown in Fig. 6 (and the analysis of many other dynamical systems such as the standard map and the Duffing oscillator, not reported in the figure) suggest that the exponent ν equals the asymptotic exponent characterizing the scaling of $\sigma_a(n)$. The existence of a constant $\alpha_{\max}$ (which is a conjecture backed up solely by numerical results) will be further used in order to derive an upper bound for the range of n within which the exponential scalings Eqs. (13) and (15) hold (see Sec. VI). It is, however, important to stress that no claim is made as regards the general validity of this conjecture. It is simply asserted that the existence of a constant $\alpha_{\max}$ has been observed and checked accurately for the dynamical systems under investigation.

B. Correlation properties and scaling of $\sigma_a(n)$

In Sec. IV A we have shown that the functional form of the high-stretching tail of $\Pi(\alpha)$ (for $\alpha>\overline{\alpha}$) depends solely on the time behavior of the variance of the elongation exponents, through the function $\zeta^{-1}(x)$. In this section we outline the main scaling properties of $\sigma_a^2(n)$ which will be useful for the purposes of this article.

Starting from Eq. (5), and after some algebra, it follows that

$$\sigma_a^2(n)=n(\langle a_1^2\rangle-\langle a_1\rangle^2)\times\left[2\sum_{k=0}^{n-1}C_{2a_1}(k)-1-\frac{2}{n}\sum_{h=0}^{n-1}hC_{2a_1}(h)\right], \tag{20}$$

where

$$C_{2a_1}(h)=\frac{\langle[a_1(\mathbf{x}_{i+h}(\mathbf{x}))-\langle a_1\rangle][a_1(\mathbf{x}_i(\mathbf{x}))-\langle a_1\rangle]\rangle}{\langle a_1^2\rangle-\langle a_1\rangle^2},$$

$$h=0,1,\ldots \tag{21}$$

is the normalized $[C_{2a_1}(0)=1]$ autocorrelation function of the one-step elongation exponents averaged over an ergodic trajectory.

According to Eq. (20), if $C_{2a_1}(h)$ is summable [i.e., if $\Sigma_{h=0}^{\infty}C_{2a_1}(h)$ is finite], then $\sigma_a^2(n)$ scales asymptotically as $\sigma_a^2(n)\simeq\sigma_0^2 n$, since the term within square brackets in Eq. (20) approaches a constant value. The summability of the

autocorrelation function $C_{2a_1}(n)$ has been proved by Ruelle [28,29] and Sinai [30] (see also [31]) for hyperbolic systems, for which the autocorrelation function of any smooth function exhibits an asymptotic exponential decay. As extensively discussed in [11], two-dimensional chaotic diffeomorphisms admit a hyperbolic structure within the chaotic region $\mathcal{C}_c$. It is therefore possible to enforce the Sinai-Ruelle theorem on the autocorrelation function of the one-step elongations, and to conclude that the linear asymptotic scaling of $\sigma_a^2(n)$ with n is a generic feature of two-dimensional chaotic diffeomorphisms.

On the other hand, several authors [32,12] have observed numerically that at intermediate-time scales ($n<n_c$, where n_c is a crossover time) $\sigma_a^2(n)$ exhibits an anomalous power-law behavior $\sigma_a^2(n)\simeq\sigma_i^2 n^{2\beta}$ with $0<\beta<1$. The crossover time n_c can be very large, depending on the correlation properties (stickiness) within the boundary layer contained in $\mathcal{C}_c$ surrounding islands of quasiperiodicity and cantori [33]. As a consequence of this observation, some authors argue that the anomalous scaling characterized by an exponent $\beta\neq 1/2$ would be a persistent feature of some dynamical systems [32,12]. For the purpose of this article [which focuses on the short- and intermediate-time behavior of the moment hierarchy $M(m;n)$], the asymptotic behavior of $\sigma_a^2(n)$ is of limited interest. However, for the sake of completeness, it is important to point out that recent numerical analysis [34] has clearly shown that for two-dimensional chaotic diffeomorphisms in which an anomalous scaling behavior of $\sigma_a^2(n)$ has been observed with an exponent $\beta\neq 1/2$ (such as the standard map for $1\leqslant T\leqslant 5$ [32] and $T=6.9115$ [12]), this phenomenon is of transient nature, and as n increases the scaling of $\sigma_a^2(n)$ converges towards the linear scaling.

To give an example of the typical crossover behavior of $\sigma_a(n)$, Figs. 7(a)–7(c) show the case of the sine flow for three different values of the parameter T. Depending on T, the crossover time n_c can vary from $n_c\simeq 1000$ ($T=0.5$) to $n_c\simeq 100$ ($T=0.6$). For $T=0.8$, asymptotic behavior sets in right from the first iterations and no crossover occurs.

This crossover behavior of $\sigma_a(n)$ had a direct counterpart in the behavior for $\zeta(n)$, Eq. (18), and consequently in its inverse function $\zeta^{-1}(x)$ entering into Eq. (17), which can be approximated by

$$\zeta^{-1}(x)=\begin{cases}(\sigma_i x)^{1/(1-\beta)} & \text{for } x<\zeta(n_c)\\ (\sigma_0 x)^2 & \text{for } x>\zeta(n_c).\end{cases} \tag{22}$$

Where no crossover occurs, we define conventionally $\sigma_i=\sigma_0$ and $\beta=1/2$.

By substituting Eq. (22) into Eq. (17), it is possible to obtain the functional dependence of $\Pi(\alpha)$ on α for $\alpha>\overline{\alpha}$. Equations (16), (17), and (22) are in fact the starting point for the analysis of the scaling behavior of the moments of the stretching field. Needless to say, the short-time behavior of $\sigma_a(n)$ is particularly important in the analysis of the short- or intermediate-time scaling of $M(m;n)$.

V. SHORT-TIME SCALING OF THE MOMENT HIERARCHY $M(m;n)$

By applying the results discussed in Sec. IV, it is possible to obtain an analytic expression for the moment hierarchy of the elongations (stretchings). This topic is developed in this section. Let $F(\lambda_e^{(n)};n)$ be the probability density function of the elongation field $\lambda_e^{(n)}$ associated with its ergodic average. The relation between $F(\lambda_e^{(n)};n)$ and $P(a_n;n)$ follows from a simple probability balance and reads as

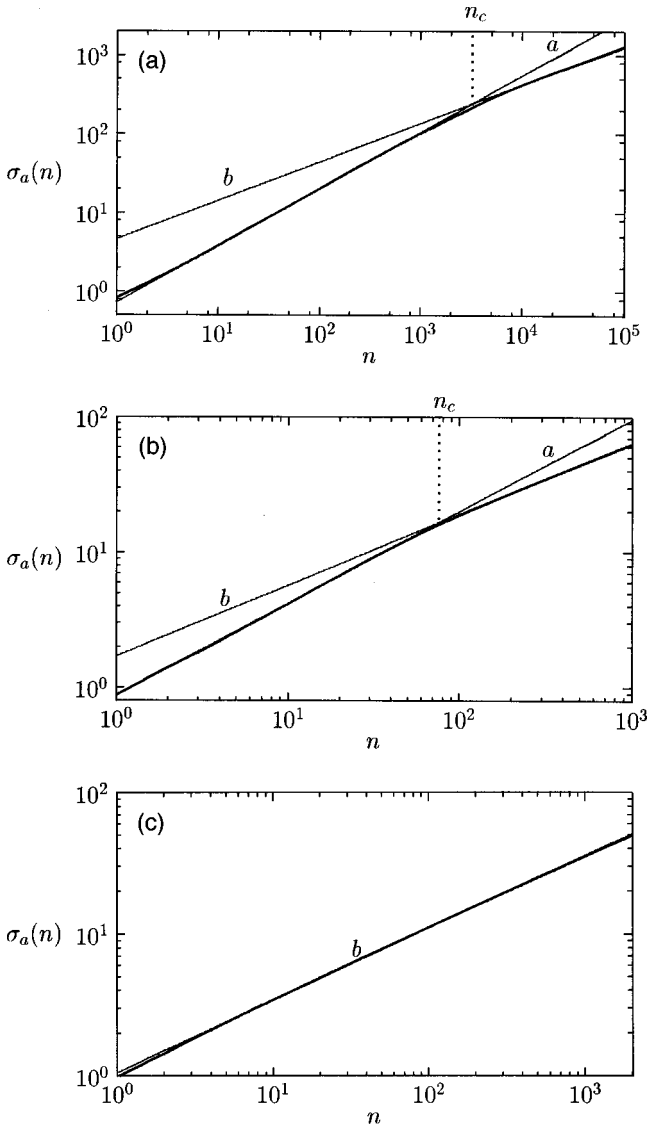

FIG. 7. Ln-ln plot of $\sigma_a(n)$ vs n for the sine flow for several values of T. (a) $T=0.5$; (b) $T=0.6$; (c) $T=0.8$. Line (a) shows the short- or intermediate-time behavior $\sigma_a(n)\sim n^{\beta}$. Line ($b$) shows the asymptotic behavior $\sigma_a(n)\sim n^{1/2}$. The dotted vertical line indicates the crossover value n_c.

$$F(\lambda_e^{(n)};n)=\frac{P(\ln\lambda_e^{(n)};n)}{\lambda_e^{(n)}}. \tag{23}$$

From the definition of the mth order moment $M(m;n)=\langle(\lambda_e^{(n)})^m\rangle$ of $\lambda_e^{(n)}$, it readily follows that

$$M(m;n)=\int_0^\infty(\lambda_e^{(n)})^m F(\lambda_e^{(n)};n)\,d\lambda_e^{(n)}$$

$$=\int_0^\infty(\lambda_e^{(n)})^{m-1}P(\ln\lambda_e^{(n)};n)\,d\lambda_e^{(n)}. \tag{24}$$

The functional form of $P(a_n;n)$, Eq. (16), can be substituted into Eq. (24), and by making use of a change of integration variable $\alpha=(\ln\lambda_e^{(n)}-n\Lambda)/\sigma_a(n)$ it follows that

$$M(m;n)=e^{nm\Lambda}\int_{-\infty}^{\infty}e^{\alpha m\sigma_a(n)}\Pi(\alpha)d\alpha. \tag{25}$$

Since $\sigma_a(n)$ is by definition positive, Eq. (25) can be manipulated to yield

$$\frac{M(m;n)}{e^{nm\Lambda}}=C+\int_0^{\infty}e^{\alpha m\sigma_a(n)}\Pi(\alpha)d\alpha=C+I(m;n), \tag{26}$$

where $C=\int_{-\infty}^{0}e^{nm\sigma_a(n)}\Pi(\alpha)d\alpha\in(0,1)$ is a positive quantity always bounded by 1. Equation (26) follows from the application of the mean-value theorem to the integral appearing in Eq. (25) restricted to the interval $(-\infty,0)$. The invariant function $\Pi(\alpha)$ is a smooth, unimodular function for $\alpha\geqslant 0$, and the integrand $e^{\alpha m\sigma_a(n)}\Pi(\alpha)$ attains a local maximum for $\alpha\in[0,\infty)$. We can therefore apply the method of steepest descent [35] to the integral appearing in Eq. (26). This gives the following estimate for $I(m;n)$:

$$I(m;n)\simeq e^{\alpha^* m\sigma_a(n)}\Pi(\alpha^*), \tag{27}$$

where $\alpha^*=\alpha^*(n,m)>0$ is the local maximum of $\exp[\alpha m\sigma_a(n)]\Pi(\alpha)$, the solution of the equation

$$\Pi(\alpha^*)m\sigma_a(n)+\frac{d\Pi(\alpha)}{d\alpha}\Big|_{\alpha=\alpha^*}=0. \tag{28}$$

Since $\exp[\alpha m\sigma_a(n)]$ is a monotonically increasing function of n for each m, it is easy to see that the unimodularity of $\Pi(\alpha)$ for positive α implies that α^* is always greater than the mode $\overline{\alpha}$ of $\Pi(\alpha)$, $\alpha^*>\overline{\alpha}$ for all n, m integers. This condition ensures that the functional expression for $\Pi(\alpha)$ in the range $(\overline{\alpha},\infty)$, obtained by merging Eqs. (17) and (22), can be properly applied to obtain

$$I(m;n)\simeq\Pi(\overline{\alpha})e^{\alpha^* m\sigma_a(n)}\exp\left[-c_1\zeta^{-1}\left(\frac{\alpha^*-\overline{\alpha}}{c_2}\right)\right], \tag{29}$$

where α^* can be expressed in closed form in terms of the two functions ζ and ζ^{-1}:

$$\frac{nm}{\zeta(n)}-\frac{c_1}{c_2}\frac{d\zeta^{-1}(x)}{dx}\Big|_{x=(\alpha^*-\overline{\alpha})/c_2}=0. \tag{30}$$

Together with the expression for $\zeta(n)$ and $\zeta^{-1}(x)$, Eq. (22), Eqs. (29) and (30) yield an analytic expression for the mth-order moment of the elongation field depending exclusively on the function $\zeta(n)$, its inverse, and the two constants c_1 and c_2 characterizing the properties of $\Pi(\alpha)$ for each dynamical system. As a consequence of Eq. (30), the scaling behavior of $M(m;n)$ can be directly inferred from the scaling properties of $\zeta^{-1}(x)$. As we are interested in the short- or intermediate-time behavior of the moment hierarchy $M(m;n)$, we can enforce Eq. (22) for the function $\zeta^{-1}(x)$ at intermediate-time scales $(n<n_c)$ to obtain

$$\alpha^*=\overline{\alpha}+Q(m)n^{1-\beta}, \tag{31}$$

where the function $Q(m)$ is given by

$$Q(m)=\left(\frac{m(1-\beta)\sigma_i}{c_1(\sigma_i/c_2)^{1/(1-\beta)}}\right)^{(1-\beta)/\beta}=\left(\frac{m(1-\beta)c_2^{1/(1-\beta)}}{c_1}\right)^{(1-\beta)/\beta}\frac{1}{\sigma_i}=\frac{K(m)}{\sigma_i}. \tag{32}$$

By substituting Eq. (32) into Eq. (29), it follows that

$$I(m;n)\simeq\Pi(\overline{\alpha})\exp[n\Gamma_1(m)+n^{\beta}\Gamma_2(m)], \tag{33}$$

where the two functions $\Gamma_1(m)$ and $\Gamma_2(m)$ are defined by

$$\Gamma_1(m)=Q(m)\sigma_i\beta m=K(m)\beta m,\quad \Gamma_2(m)=\overline{\alpha}\sigma_i m. \tag{34}$$

The constant C entering into Eq. (26) is bounded by 1 and can be overlooked as compared to the exponential term $I(m;n)$. By collecting together Eqs. (33) and (34) and substituting them into Eq. (26), we thus arrive at the estimate for $M(m;n)$ given by

$$M(m;n)\simeq\Pi(\overline{\alpha})\exp\{n[m\Lambda+\Gamma_1(m)]+n^{\beta}\Gamma_2(m)\}. \tag{35}$$

Let us now analyze the implications of Eq. (35) in greater depth. The first and most important result is that the mth-order moments $M(m;n)$ for $m=1,2,\ldots$ scale with n faster than $\exp(nm\Lambda)$, since both $\Gamma_1(m)$ and $\Gamma_2(m)$ are always greater than or equal to zero. However, apart from the case where $\overline{\alpha}=0$, which implies by Eq. (34) $\Gamma_2(m)=0$, the short-time behavior of $M(m;n)$ is not strictly exponential, due to the presence of the stretched exponential contribution $\exp[n^{\beta}\Gamma_2(m)]$. This means that in the general case, the exponential expressions, Eqs. (13) and (15), should be regarded simply as a good, and sometimes very good, approximation of the short-time scaling. The case $\overline{\alpha}>0$ often occurs in the presence of significantly asymmetric $\Pi(\alpha)$, as can be observed from Fig. 4. In the case $\overline{\alpha}>0$, since $\Gamma_2(m)$ is a linearly increasing function of σ_i [while $\Gamma_1(m)$ does not depend explicitly on σ_i], the greater the value of σ_i (i.e., the broader the distribution of elongation exponents), the faster the short-time growth of the intermaterial length $L^{(n)}$ and of the higher-order moments $M(m,n)$, compared to limit predicted by the Liapunov exponent.

A particular case is represented by the family of K diffeomorphisms on the torus. For these systems, as already discussed in Sec. III, $\sigma_a(n)=\sigma_K+o(n)\geqslant 0$ is definitely a constant and all the moments $M(m;n)$ follow the exponential homogeneous scaling induced by the Liapunov exponent, $M(m;n)\sim\exp(nm\Lambda)$. This result follows directly from Eqs. (25) and (26) since the term $I(m;n)$ does not depend explicitly on the time n.

From the observations discussed above, it follows that the short-time deviation from the exponential behavior $\exp(nm\Lambda)$ can be regarded as a measure of the dynamic heterogeneity of the elongation field as it is directly related to the properties of the variance $\sigma_a^2(n)$. Beigie *et al.* [1] at-

tribute this deviation, in the case $m=1$, to the non-Gaussian nature of the stretching distribution. Although it is certainly true that the non-Gaussian behavior of $\Pi(\alpha)$ influences the scaling of the moment hierarchy $M(m;n)$, the conclusion envisaged in [1] is not of general validity. Indeed, also in the case of a Gaussian $\Pi(\alpha)$, the length of a generic material line can grow at short times with an exponent definitely larger than Λ. To check this assertion, let us consider a square-exponential behavior for $\Pi(\alpha)=\Pi(\bar{\alpha})\exp(-k\alpha^2)$ (coinciding with a Gaussian shape for $k=1/2$). This case implies $\bar{\alpha}=0$, $\beta=1/2$, and $k=c_1/(c_2\sigma_i)^2$. By substituting these values into Eq. (35) it follows that

$$M(m;n)\sim\exp\left[n\left(m\Lambda+\frac{\sigma_i^2 m^2}{4k}\right)\right]. \tag{36}$$

A short-time deviation from the Liapunov scaling can therefore occur also in the strictly Gaussian case ($k=1/2$) since σ_i is nonzero. As mentioned above, the main factor affecting deviation from the Liapunov scaling would appear to be the heterogeneity in the distribution of the stretching exponents (i.e., a nonzero value of σ_i), rather than the non-Gaussian feature of the associated probability density function.

VI. COMPARISON WITH NUMERICAL RESULTS

One important issue remaining after the analysis developed in Sec. V is the definition of the range of temporal validity of Eq. (35). This topic is analyzed in this section, which also compares Eq. (35) with the results of numerical simulations.

The explicit expression of α^* as a function of m and n, Eq. (31), enables us to derive some general properties as regards the n range of applicability of Eq. (35) and the quantitative meaning of the short or intermediate scaling for $M(m;n)$. The steepest-descent approximation of the integral $I(n,m)$ Eq. (27) makes sense as long as the local maximum α^* defined in Eq. (31) is smaller than the finite upper bound $\alpha_{\max}$. The validity of Eq. (31) is therefore limited by the condition $\alpha^*<\alpha_{\max}$. Since α^* depends explicitly on the time n, this condition can be recast into an equivalent condition for the time range up to which Eq. (35) holds, i.e.,

$$n<n^*=\left(\frac{\alpha_{\max}-\bar{\alpha}}{Q(m)}\right)^{1/(1-\beta)}. \tag{37}$$

The value n^* can be taken not only as the upper bound for the applicability of the steepest-descent method [i.e., for Eq. (35)], but also as a quantitative definition of the concept of short- or intermediate-time scaling.

Since $\beta<1$, and $Q(m)$ is a monotonically increasing function of m, the bound n^* is a monotonically decreasing function of the order m. The range of applicability of Eq. (35) and the concept of short- or intermediate-time scaling therefore depend on m, and their validity is restricted in practice to the lower-order moments ($m=1,2,3$). This result is in agreement with the numerical results as can be observed from the comparison of the short-time scaling of the three lower-order moments shown in Fig. 3.

Let us now compare Eq. (35) with numerical simulations. Figure 8 shows the excellent agreement between numerical

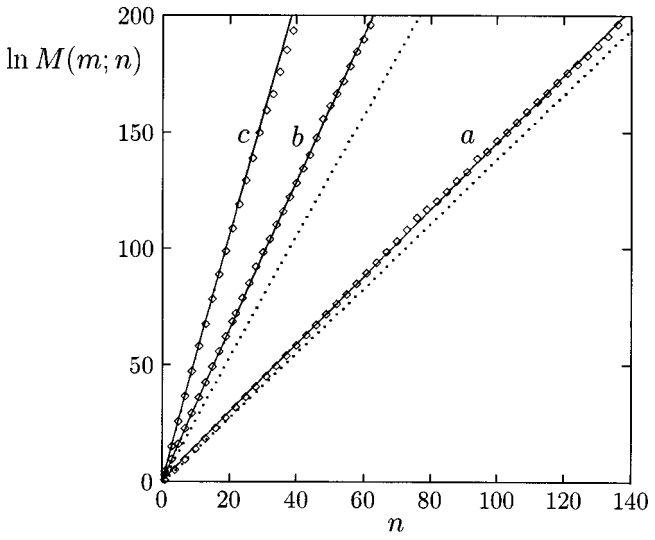

FIG. 8. $\ln M(m;n)$ vs n (dots) for the sine flow ($T=0.5$) compared with the theoretical expression Eq. (35). (*a*) $m=1$; (*b*) $m=2$; (*c*) $m=3$. The dotted lines are the predictions based on Eq. (35), with the stretched exponent contribution overlooked [i.e., $\Gamma_2(m)=0$] for $m=1$ and $m=2$.

results for $M(1;n)$, $M(2;n)$, and $M(3;n)$ for the sine flow ($T=0.5$) and the theoretical prediction Eq. (35). It is important to point out that all the parameters, σ_i, β and c_1, c_2 and $\Pi(\alpha)$, entering into Eq. (35) have been independently obtained, respectively, from the scaling of $\sigma_a(n)$ and from the interpolation of $\Pi(\alpha)$ with the theoretical expression Eqs. (17) and (22). In this case, $\alpha_{\max}\simeq 2.0$ and the n range of applicability of Eq. (35) is significantly large: $n^*(m=1)\simeq 180$, $n^*(m=2)\simeq 60$, and $n^*(m=3)\simeq 35$.

The case of the sine flow for $T=0.5$ is particularly interesting from the point of view of the scaling, since the function $\Pi(\alpha)$ exhibits a value of $\bar{\alpha}$ which is significantly greater than zero, namely, $\bar{\alpha}\simeq 0.34$, and the factor $\Gamma_2(m)$ related to the stretched exponential contribution is of the same order of magnitude as the factor $\Gamma_1(m)$ of the strictly exponential scaling. In this case, the stretched exponential term $\exp[n^\beta\Gamma_2(m)]$ makes a significant contribution to the initial scaling. This is made evident in Fig. 8, where the dotted lines show the functional behavior of Eq. (35), with the stretched exponential term fictitiously set equal to zero [i.e., $\Gamma_2(m)=0$].

Although Eq. (35) does not predict a strictly exponential behavior for $\langle(\lambda_e^{(n)})^m\rangle$, an exponential fitting of numerical data furnishes a good approximation of the short-time behavior, as already discussed in Sec. II. It is reasonable to approximate the scaling of $M(m;n)$ with an exponential behavior $\exp[n\theta_p(m)]$, in which $\theta_p(m)$ is an effective scaling exponent. As for any effective quantity, the definition of $\theta_p(m)$ is subject to a certain degree of arbitrariness. We define $\theta_p(m)$ as the value of the derivative of $\ln M(m;n)$ at the midpoint $n_p(m)=n^*(m)/2$ of its range of applicability defined by Eq. (37), i.e.,

$$\theta_p(m)=\left.\frac{d\ln M(m;n)}{dn}\right|_{n=n_p(m)}$$

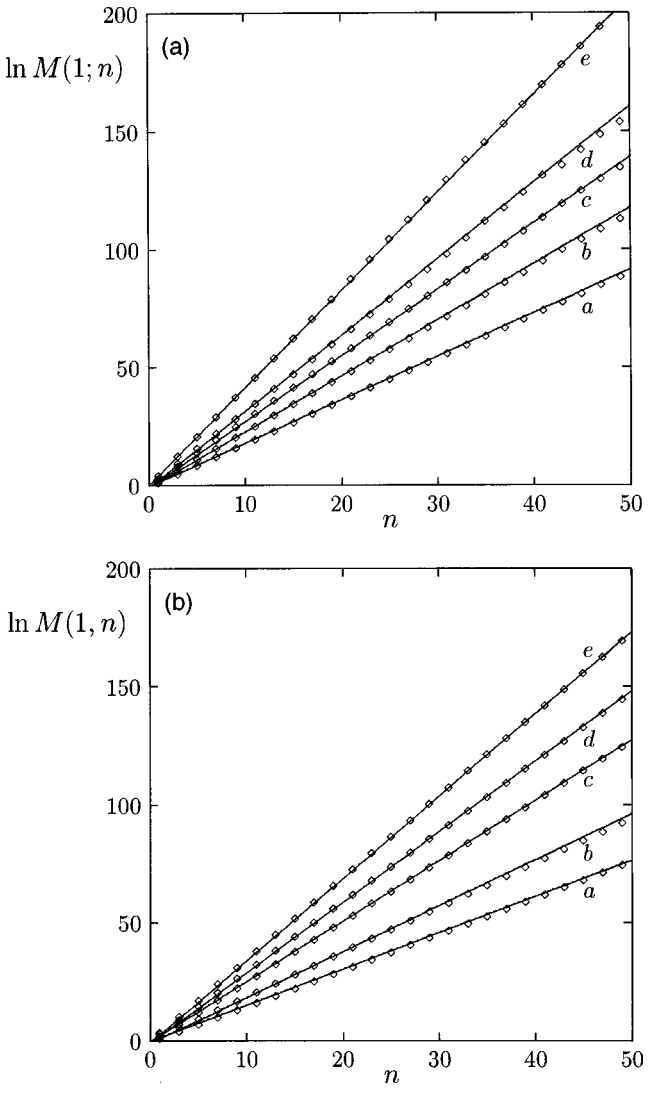

FIG. 9. $\ln M(1;n)$ vs n for several values of T (dots) compared with the exponential behavior $M(1;n)\sim\exp(n\theta_p)$ (lines) with $\theta_p=\theta_p(1)$ given by Eq. (37). (a) Sine flow, $T=0.6,0.8,1.0,1.2,2.0$. (b) Standard map, $T=6.9115,10,20,30,50$.

$$=m\Lambda+\Gamma_1(m)+\Gamma_2(m)\beta n_p^{\beta-1}. \tag{38}$$

This criterion for $\theta_p(m)$ gives good scaling predictions, i.e.,

$$\exp\{[m\Lambda+\Gamma_1(m)]n+\Gamma_2(m)n^{\beta}\}\simeq\exp[n\theta_p(m)]$$

$$\text{for } n<n^*. \tag{39}$$

To give a numerical example, Fig. 9 shows the good level of agreement between numerical simulations and the effective exponential approximation based on $\theta_p(1)$, obtained theoretically from Eqs. (35) and (38), for the sine flow and the standard map for different values of the parameters. In order to summarize the extensive numerical analysis performed, Fig. 10 compares the exponent $\theta=\theta(1)$ obtained from the analysis of the ergodic averages of the elongation exponent and the effective exponent $\theta_p=\theta_p(1)$ for several dynamical systems (Duffing oscillator and standard map) and chaotic flows (sine flow and flow between two eccentric cylinders). The agreement is satisfactory and the maximum deviation is less than 5%.

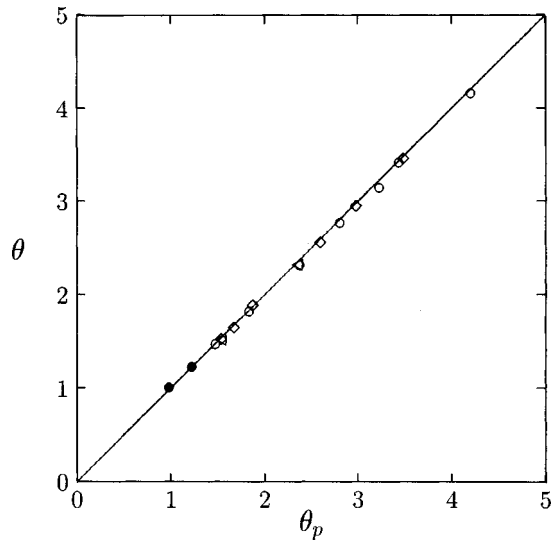

FIG. 10. θ vs $\theta_p=\theta_p(1)$ given by Eq. (37) for several dynamical systems and several sets of parameters. ●: Duffing oscillator, $\omega=1.0$, $\varepsilon=0.75,2.35$; ◁: flow between eccentric cylinders, $\theta_{\text{out}}=2\pi,5\pi/2$; ◇: standard map, $T=6.9115,8,10,20,30,50$; ○: sine flow, $T=0.5,0.6,0.8,1.0,1.2.1.4,2.0$.

We therefore conclude that the theoretical analysis based on Eq. (35) is fully predictive and yields accurate values for the short- or intermediate-time scaling of the intermaterial contact length $L^{(n)}$ and of the entire moment hierarchy $M(m;n)$.

VII. ASYMPTOTIC SCALING OF $M(m;n)$

As a final issue, let us consider the asymptotic scaling of $M(m;n)$ for differentiable dynamical systems in order to highlight the influence of the variance $\sigma_a(n)$.

As discussed in the Introduction, the application of the Oseledec theorem to diffeomorphisms implies that

$$\lim_{n\to\infty}\frac{1}{n}\ln M(m;n)=m\Lambda, \tag{40}$$

i.e., the dominant contribution to the asymptotic scaling of the stretching hierarchy $M(m;n)$ is made by the Liapunov factor $\exp(nm\Lambda)$. This result would suggest that for very long time, independently of the initial scaling, the asymptotic behavior of $M(m;n)$ is exclusively controlled by the Liapunov exponent, and *a fortiori*, the intermaterial contact length $L^{(n)}$ would definitely grow as $\exp(n\Lambda)$.

This conclusion is not in fact completely correct, and apart from the dominant Liapunov scaling, there exists a second-order but significant correction depending on the variance $\sigma_a^2(n)$. Let us take Eq. (25) as our starting point to highlight this additional effect. The support upon which $\Pi(\alpha)$ is defined admits, for each n, an upper bound $\alpha_{\max}^{(n)}$ given by Eq. (19).

Since $\Pi(\alpha)$ is in general a smooth and continuous function of its argument, we can apply the mean-value theorem to Eq. (25) to obtain

$$M(m;n)=e^{nm\Lambda}\int_{-\infty}^{\alpha_{\max}^{(n)}}e^{\alpha m\sigma_a(n)}\Pi(\alpha)\,d\alpha$$

$$=\tilde{\Pi}e^{m\Lambda n}\int_{-\infty}^{\alpha_{\max}^{(n)}}e^{\alpha m\sigma_a(n)}d\alpha$$

$$=\frac{\tilde{\Pi}e^{nm\Lambda}}{m\sigma_a(n)}e^{\alpha_{\max}^{(n)}m\sigma_a(n)}, \tag{41}$$

where $\tilde{\Pi}\in(0,\Pi(\overline{\alpha}))$.

By Eq. (19), $\alpha_{\max}^{(n)}\sigma_a(n)<Cn^{\nu}$, where C is a constant and ν a positive exponent strictly less than 1. The condition $\nu<1$ ensures that Eq. (40) is satisfied. On the other hand, Eq. (41) implies that the asymptotic scaling of $M(m;n)$ is the result of two main contributions: the exponential Liapunov scaling and a stretched exponential contribution with an exponent $\nu<1$ which depends on $\sigma_a(n)$.

In the particular case where $\alpha_{\max}^{(n)}$ is a constant independent of n, as numerically observed for several dynamical systems (see Fig. 6), Eq. (41) reduces to

$$M(m;n)\sim e^{nm\Lambda+\alpha_{\max}m\sigma_a(n)}\sim e^{nm\Lambda+n^{1/2}m\sigma_0}, \tag{42}$$

in which we use the asymptotic scaling of $\sigma_a(n)$ discussed in Sec. IV B.

Two main conclusions can be drawn from Eqs. (41) and (42). The intermaterial contact length $L^{(n)}$ grows asymptotically faster than $\exp(n\Lambda)$ by a factor $\exp(n^{1/2}m\sigma_0)$. Moreover, as regards the short- or intermediate-time scaling discussed in Sec. V, the asymptotic scaling of $M(m;n)$, and *a fortiori* of $L^{(n)}$, depends on and is enhanced by the heterogeneity of the stretching distribution, expressed quantitatively by the square root of the variance $\sigma_a(n)$. This result is by no means surprising in view of the fact that the high-stretching tail of $\Pi(\alpha)$ is entirely controlled by the behavior of $\sigma_a(n)$ through the functions ζ and ζ^{-1}.

VIII. CONCLUSIONS

This article develops a scaling theory for the hierarchy of stretching moments $M(m;n)$ in the case of two-dimensional chaotic area-preserving diffeomorphic maps. The case $m=1$ is particularly interesting as regards the applications to chaotic fluid mixing since it is directly related to the rate of growth of the intermaterial contact length, which controls transport and reactive phenomena in the fluid system.

It has been shown that at short- or intermediate-time scales, the hierarchy $M(m;n)$ is characterized by an enhanced exponential scaling, the effective exponent of which is greater than $m\Lambda$.

By making use of the invariant rescaling of the probability distribution of the stretching exponents proposed recently in [9], we are able to derive the short-time scaling of $M(m;n)$, Eq. (35), and to determine the temporal range $n\in(1,n^*)$, Eq. (37), for which this scaling occurs. Equation (35) is a fully predictive relation for the short-time behavior of $M(m;n)$, as shown numerically for several characteristic model systems, and for a broad range of parameters characterizing these systems. All the quantities appearing in Eq. (35) can be obtained independently from the analysis of the variance of the stretching exponents $\sigma_a^2(n)$ and from their invariant distribution $\Pi(\alpha)$.

Our analysis of the short-time behavior, and also of the long-time properties (addressed in Sec. VII), reveals that the rate of growth of the intermaterial contact perimeter is affected by the heterogeneity in the stretching dynamics expressed by the variance $\sigma_a^2(n)$ of the stretching exponent field. This phenomenon is not only interesting in itself, but may give rise in the future to some practical implications in the improvement of mixing performances in fluid-mixing systems.

Another significant effect controlling the short- or intermediate-time scaling of $M(m;n)$ is related to the asymmetry of the invariant distribution $\Pi(\alpha)$, expressed qualitatively by its mode $\overline{\alpha}$. For $\overline{\alpha}=0$, which corresponds to a fairly symmetric case, the initial scaling is strictly exponential, and the exponent $\theta(m)$ is given by $m\Lambda+\Gamma_1(m)$. For $\overline{\alpha}>0$, which corresponds to highly asymmetric distribution of the stretching exponents (see, e.g., Fig. 4), the initial scaling of $M(m;n)$ is not strictly exponential, since a stretched exponential factor also appears, given by $\exp[n^{\beta}\Gamma_2(m)]$. An approximate (effective) exponential scaling can, however, be defined also in this case, as developed in Sec. VI, Eq. (38).

ACKNOWLEDGMENTS

This work was funded by a NSF grant (Grant No. CTS 94-14460) to F.J.M. and by an Italian MURST grant to A.A. and M.G.

[1] D. Beigie, A. Leonard, and S. Wiggins, Phys. Rev. Lett. **70**, 275 (1993).

[2] D. Beigie, A. Leonard, and S. Wiggins, Chaos Solitons Fractals **4**, 749 (1994).

[3] M. M. Alvarez, F. J. Muzzio, A. Adrover, and S. Cerbelli, in *Fractals in Engineering*, edited by J. Levy Vehel, E. Lutton, and C. Tricot (Springer-Verlag, Berlin, 1997), p. 323; M. M. Alvarez, F. J. Muzzio, S. Cerbelli, A. Adrover, and M. Giona (unpublished).

[4] J. M. Ottino, *The Kinematics of Mixing: Stretching, Chaos and Transport* (Cambridge University Press, Cambridge, England, 1989).

[5] F. J. Muzzio, P. D. Swanson, and J. M. Ottino, Phys. Fluids A **3**, 822 (1991).

[6] E. Ott and T. M. Antonsen, Jr., Phys. Rev. A **39**, 3660 (1989); F. Varosi, T. M. Antonsen, Jr., and E. Ott, Phys. Fluids A **3**, 1017 (1991).

[7] S. Wiggins, *Chaotic Transport in Dynamical Systems* (Springer-Verlag, Berlin, 1992).

[8] V. Rom-Kedar, A. Leonard, and S. Wiggins, J. Fluid Mech. **214**, 347 (1990); D. Beigie, L. Leonard, and S. Wiggins, Nonlinearity **4**, 775 (1991); R. Camassa and S. Wiggins, Phys. Rev. A **43**, 774 (1991).

[9] A. Adrover, M. Giona, and F. J. Muzzio (unpublished).

[10] V. I. Oseledec, Trans. Moscow Math. Soc. **19**, 197 (1968).
[11] M. Giona, A. Adrover, S. Cerbelli, M. M. Alvarez, and F. J. Muzzio (unpublished).
[12] T. Horita, H. Hata, R. Ishizaki, and H. Mori, Prog. Theor. Phys. **83**, 1065 (1990); H. Mori, H. Hata, T. Horita, and T. Kobayashi, Prog. Theor. Phys. Suppl. **99**, 1 (1989).
[13] Y. Elskens, Physica D **100**, 142 (1997).
[14] M. Liu, F. J. Muzzio, and R. L. Peskin, Chaos Solitons Fractals **4**, 869 (1994).
[15] B. V. Chirikov, Phys. Rep. **52**, 265 (1979).
[16] J. M. Greene, J. Math. Phys. **20**, 1183 (1979).
[17] J. Guckenheimer and P. Holmes, *Nonlinear Oscillations, Dynamical Systems, and Bifurcations of Vector Fields* (Springer-Verlag, Berlin, 1983).
[18] P. D. Swanson and J. M. Ottino, J. Fluid Mech. **213**, 227 (1990).
[19] G. H. Wannier, Q. Appl. Math. **VIII**, 1 (1950).
[20] D. V. Anosov amd V. V. Solodov, in *Dynamical Systems IX*, edited by D. V. Anosov, Encyclopaedia of Mathematical Sciences Vol. 66 (Springer-Verlag, Berlin, 1995), pp. 10–92; V. I. Arnold, *Geometrical Methods in the Theory of Ordinary Differential Equations* (Springer-Verlag, Berlin, 1983).
[21] H. G. E. Hentschel and I. Procaccia, Physica D **8**, 435 (1983).
[22] J. D. Farmer, E. Ott, and J. A. Yorke, Physica D **7**, 153 (1983).
[23] J. P. Eckmann and D. Ruelle, Rev. Mod. Phys. **57**, 617 (1985).
[24] D. F. Escande, Phys. Rep. **3-4**, 165 (1985).
[25] R. Livi, M. Pettini, S. Ruffo, M. Sparpaglione, and A. Vulpiani, Phys. Rev. A **31**, 1039 (1985); R. Livi, M. Pettini, S. Ruffo, and A. Vulpiani, *ibid.* **31**, 2740 (1985); R. Livi, A. Politi, S. Ruffo, and A. Vulpiani, J. Stat. Phys. **46**, 147 (1987).
[26] P. Grassberger, R. Badii, and A. Politi, J. Stat. Phys. **51**, 135 (1988).
[27] M. A. Sepulveda, R. Badii, and E. Pollak, Phys. Rev. Lett. **63**, 1226 (1989).
[28] D. Ruelle, Phys. Rev. Lett. **56**, 405 (1986).
[29] D. Ruelle, J. Stat. Phys. **44**, 281 (1986).
[30] Y. Sinai, Russ. Math. Surveys **27**, 21 (1972).
[31] V. Baladi, J-P. Eckmann, and D. Ruelle, Nonlinearity **2**, 119 (1989).
[32] H. Kantz and P. Grassberger, Phys. Lett. A **123**, 437 (1987).
[33] B. V. Chirikov and D. L. Shepelyansky, Physica D **13**, 395 (1984).
[34] A. Adrover and M. Giona, Physica A (to be published).
[35] M. Born and E. Wolf, *Principles of Optics* (Pergamon Press, Oxford, 1980), p. 747.